Photocatalytic activity of pure rutile particles derived from a photo-assisted sol-gel method

Haimei Liu, Wensheng Yang, Ying Ma, Xianfu Ye and Jiannian Yao*

Center for Molecular Science, Institute of Chemistry, The Chinese Academy of Sciences, Beijing 100080, P. R. China. E-mail: jnyao@infoc3.icas.ac.cn

Received (in Montpellier, France) 23rd October 2002, Accepted 2nd December 2002
First published as an Advance Article on the web 12th February 2003

Pure rutile titania was prepared at a calcination temperature of 600 °C by using a photo-assisted sol-gel method. Compared with the traditional sol-gel method the photo-irradiation introduced into the colloid preparation process can accelerate the phase transformation from the anatase to rutile phase. Moreover, it was found that the as-prepared rutile powder samples exhibited a regular polyhedron shape and small grain size distribution. These rutile particles showed a remarkable photocatalytic activity in decomposing organic pollutants under ultraviolet irradiation. The photocatalytic degradation rates of rutile particles in aqueous solution were correlative with not only the grain surface area but also the particle agglomeration state.

Introduction

Semiconductor photocatalysts have attracted much attention due to their applicability in the treatment of wastes and pollutants in air and water.[1–5] Among them, titanium dioxide (TiO_2) has been most often used because of its chemical stability and excellent photocatalytic activity. It is well-known that TiO_2 has three polymorphs: rutile (tetragonal, $P4_2/mnm$), anatase (tetragonal, $I4_1/amd$), and brookite (orthorhombic, $Pcab$). Anatase TiO_2 is believed, on the basis of the results of many experiments, to be more active than rutile,[6–8] while several reports claimed that rutile showed higher activity for specific types of photocatalytic reactions.[9] It has also been reported that the difference between rutile and anatase photosensitization does not originate from the different positions of the conduction band and valence band edges. The very low activity of either neat or modified rutile is due to adsorption properties and charge carrier lifetime instead of redox features.[10,11] Usually rutile powders are produced at high calcination temperatures, for example, Balachandran and Eror have reported that anatase transforms into the rutile phase at 750 °C due to a fine crystallite size;[12] Ding and Qi have also reported that anatase did not transform to rutile until the annealing temperature was increased to 800 °C;[13] Robert *et al.* have demonstrated that single crystals of anatase were transformed into rutile at 900–950 °C, which resulted from a perferred orientation of the product.[14] The pure rutile particles prepared at such high calcination temperatures consequentially exhibit large grain sizes and small surface areas, which result in their poor adsorption of active species and low photocatalytic activity.

Recently we found that under ultraviolet light irradiation ($\lambda > 290$ nm) of TiO_2 colloids during a sol-gel preparation process the phase transition temperature (PTT) from amorphous to anatase was decreased by nearly 100 °C compared with that of the traditional sol-gel method. Our early work[15] confirmed that oxygen vacancies induced by ultraviolet illumination promoted the phase transformation of TiO_2 powders. In this paper we synthesized rutile titania by using the same photo-assisted sol-gel method and found that the PTT of anatase-to-rutile was decreased to 600 °C. The rutile powders prepared by such a photo-assisted sol-gel method showed small grain sizes and relatively large specific surface areas.

Furthermore, we used rhodamine B and 2,4-dichlorophenol as target pollutants to investigate the photocatalytic activity of these rutile powders under UV irradiation. The experimental results revealed that the specific surface area of the catalyst in the decomposition reaction was not the crucial factor for its high activity but that the surface properties and agglomerated state of the samples played a key role during the photocatalytic process.

This study may provide an alternative approach for enhancement of photocatalytic activity of pure rutile powders in the decomposition of organic pollutants in aqueous solutions.

Experimental section

Materials preparation

Two sets of titania colloids were prepared in the same manner as described elsewhere.[15] The major and only difference between the two colloids was that one system was UV-irradiated and the other was not. Titanium isopropoxide, Ti-$(OC_3H^i_7)_4$(Acros, >98%), was used as the titanium precursor in the sol-gel process. Other chemicals and solvents were of reagent grade and used without further purification. In a typical synthesis 5.0 ml titanium isopropoxide was first dissolved in 10 ml of propyl alcohol and the solution was then slowly dropped into 40 ml of an ethanol solution containing 2.5 ml hydrochloride acid and 1.5 ml deionized water under vigorous stirring. The mixture was illuminated for about 8 h before the solvent evaporation. The solvent of the TiO_2 colloids was allowed to evaporate from the system at room temperature and then the dry gel was calcined at various temperatures to obtain the powder samples. The samples prepared by the photo-irradiated method are denoted as P-sample, such as P-400 (annealed at 400 °C) and so on, while the other set of non-irradiated samples are identified as N-sample.

Photocatalytic degradation

Rhodamine B (RB) was from Tokyo Kasei Kogyo Co., Ltd.; 2,4-dichlorophenol (2,4-DCP) was from Beijing Chemical Co. and was used without further purification. An aqueous suspension of a dye (2.0×10^{-5} M, 50 ml) and TiO_2 (10 mg)

was contained in an 80 ml Pyrex glass vessel and was stirred about 30 min in the dark to reach the adsorption/desorption equilibrium. Subsequently the dispersion was irradiated under air-equilibrated conditions with ultraviolet light. The UV irradiation was provided by a 500 W high-pressure mercury lamp and passed through a 1.0 cm thick circulating water cuvette to remove the heating IR beams. After irradiation a 4 ml aliquot was taken at various intervals and the TiO_2 powder was separated off from the reaction mixture by centrifuging, then variations in the concentration of the dye in the degraded solution were monitored by UV-Vis spectroscopy (Shimadzu UV-1601PC). The characteristic absorption bands at *ca.* 554 nm for RB and *ca.* 284 nm for 2,4-DCP were monitored during the degradation process.

Characterization

The powder X-ray diffraction patterns were collected with CuKα radiation ($\lambda = 1.5406$ Å) of 50 kV and 300 mA at a scan rate of 0.02° per 0.12 s. The evolution of the transformation of anatase to rutile was calculated using the ratios of areas under background-subtracted {101} anatase and {110} rutile peaks.[16] The Raman spectra were taken in the backscattering geometry using the 514.5 nm line of an Ar ion laser as the excitation source with a Renishaw-2000 Raman spectrometer, and the spectral resolution and accuracy of the Raman shift are estimated to be ~2 cm^{-1}. The morphology of the synthesized powders was observed with SEM (JSM-6301F). The BET surface area of the samples, which were degassed at 473 K for 2 h, was measured by the adsorption of N_2 molecules at 77 K.

Results and discussion

It is obvious that photo-irradiation of the TiO_2 colloid accelerated the phase transformation behavior of anatase to rutile. Fig. 1 shows the XRD patterns of this process for P-samples [Fig. 1(a)] and N-samples [Fig. 1(b)]. As it can be seen, the PT reaction occurred at 450–600 °C for the former and at 550–700 °C for the latter; thus, the PTT of anatase to rutile decreased 100 °C for the UV-irradiated set of powder samples compared to the non-irradiated ones. The sharper and narrower diffraction peaks imply an increase of the particle size with increase of the calcination temperature. Moreover, Table 1 presents the rutile phase content at various temperatures during this process. At 600 °C anatase is completely transformed into rutile in the P-samples while only 48% of anatase was transformed in the N-samples at the same temperature.

Fig. 2 compares the Raman spectra of two sets of the samples during the PT process of anatase to rutile. In the UV-irradiated set [Fig. 2(a)] the distinct bands at 144, 393, and 638 cm^{-1} at 450 °C are all ascribed to the anatase phase due to the $E_g + B_{1g} + (A_{1g} + B_{1g}) + E_g$ vibrational modes of Raman activity. As the calcination temperature increase to 500 °C, a new band at 446 cm^{-1} attributed to the rutile phase appeared, indicating that the PT reaction took place. With increasing temperature three other characteristic bands of rutile at 143, 230, and 608 cm^{-1} were also apparent, in addition to an increase in the intensity of the 446 cm^{-1} band, while the band intensity of anatase gradually decreased. The characteristic bands of anatase completely disappeared at 600 °C and rutile was the only phase observed, which implied that the PT reaction occurred in the 450–600 °C range, in good agreement with the XRD results. Compared with the UV-irradiated set, the PT reaction of the non-irradiated set occurred at 550–700 °C [Fig. 2(b)], 100 °C higher than in the irradiated samples.

The preparation-induced surface morphology difference in powders of the two sets was also clearly seen from their SEM pictures. Fig. 3(a,b) show the morphology and shapes

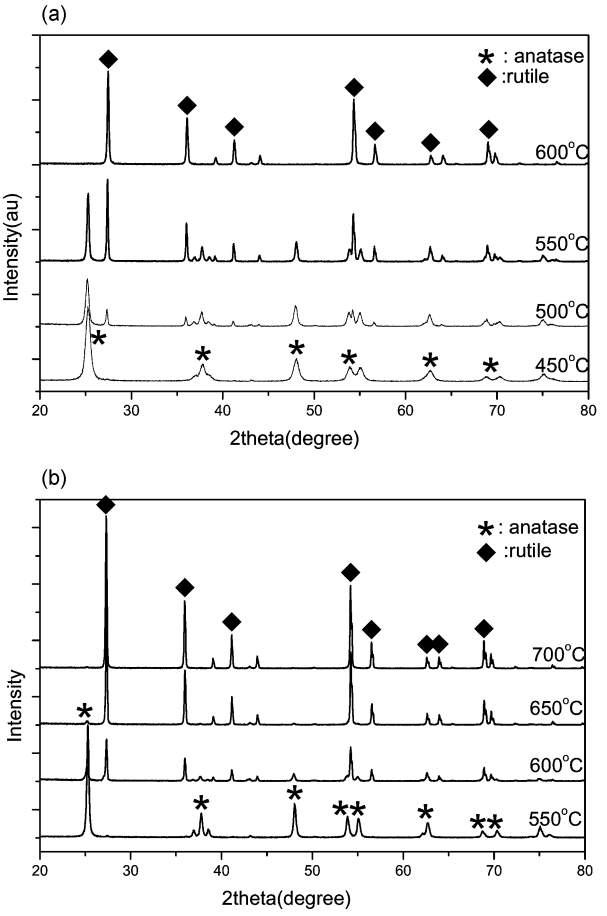

Fig. 1 The XRD patterns of the transformation process of TiO_2 powders prepared with (a) and without (b) UV irradiation.

of P-500 and P-600, respectively. These particles were regular polyhedron and did not agglomerate. Moreover, the particle size distribution was relatively narrow at 100–200 nm. As a rule, the size ratio of the largest particle to the smallest particle was < 2. In contrast, the N-500 and N-600 samples [Fig. 3(c,d)] show a much different morphology. These particles are irregular, deformed and agglomerated. The grain size is not uniform; some larger grains are surrounded by small ones. The particle size distribution is estimated to be 200–500 nm, and the size ratio of the largest particle to the mean size is > 3. This grain size inhomogeneity demonstrates the discontinuous grain growth.

Table 2 shows the BET surface areas of these samples. As can be seen, the difference in surface areas of two sets of samples, even at the same calcination temperature, is significant. For the P-sample S_{BET} is 32 $m^2\ g^{-1}$ while that for the N-sample is 2.5 $m^2\ g^{-1}$ at 600 °C; that is the former is more than ten times as large as the latter. This difference most likely results from the different agglomeration state of the two sets of particles.

Table 1 Rutile phase content of powder samples at different temperatures (°C)

	Rutile phase content (%)					
T/°C	450	500	550	600	650	700
UV-irradiated	0	29.7	66.8	100	–	–
Non-irradiated	–	0	9.5	48.3	95	100

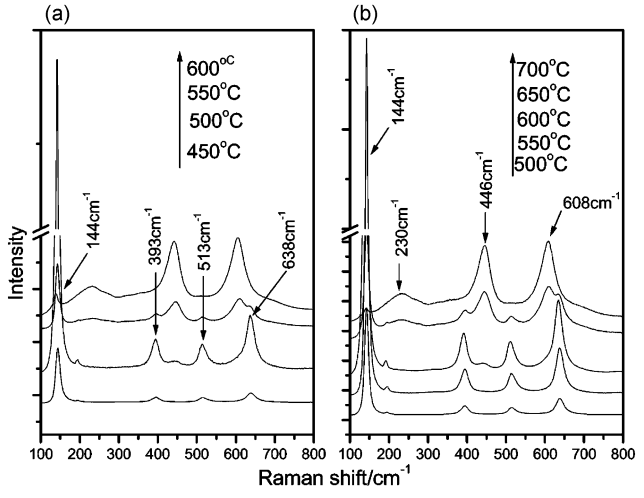

Fig. 2 The Raman spectra of TiO_2 powders at various temperatures prepared with (a) and without (b) UV irradiation.

Finally, we evaluate the photocatalytic activity of these TiO_2 samples by decomposing the organic dye molecule rhodamine B (RB), a dye often used as a tunable laser dye because of its stable photochemical properties.[17] The degradation results are depicted in Fig. 4. It is clearly shown that the photolysis of RB under the used conditions is very slight (blank) and thus the excitation of the dye can be neglected compared with the excitation of TiO_2. For the P-600 sample 90% of the dye molecules in an TiO_2 aqueous dispersion was degraded within 50 min while only 20% of the dye was degraded for N-600 after 80 min of UV irradiation. The most interesting thing is that although the BET surface area of N-500 (69 $m^2\ g^{-1}$) is larger than that of P-600 (32 $m^2\ g^{-1}$), the degradation rate of the former is slower than that of the latter. The degradation rate of P-400 was rather equivalent to that of P25, which is ascribed to its high surface area of 158 $m^2\ g^{-1}$. Similar results were also observed in the degradation of 2,4-DCP, shown in Fig. 5. For the N-600 sample no obvious change of absorption spectra can be observed while for the P-600 sample, approximately 30% of 2,4-DCP was decomposed during the 180 min irradiation time. However, the degradation rates of P-500 and P-400 were very similar although their BET surface areas were different in value (Table 2).

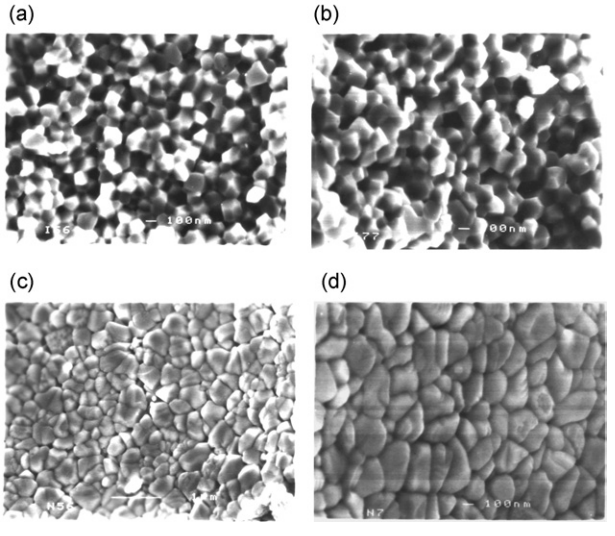

Fig. 3 Field emission SEM pictures of TiO_2 powder samples annealed at different temperatures: (a) P-sample, 500 °C; (b) P-sample, 600 °C; (c) N-sample, 500 °C; (d) N-sample, 600 °C.

Table 2 The special surface areas of powder samples at various temperatures (°C)

	$S_{BET}/m^2\ g^{-1}$		
T/°C	400	500	600
P-samples	158	103	32
N-samples	76	69	2.5

Generally, the smaller the surface areas the poorer the photocatalytic activity of powder samples, but in our present work this factor is not the most important and crucial factor. It is well-accepted[18–20] that the photocatalytic activity of suspended TiO_2 in solution strongly depends on the physical properties of TiO_2 (*e.g.*, crystal structure, surface area, surface hydroxyls and particle size) and operating conditions (*e.g.*, light intensity, oxygen, initial concentration of chemicals, amount of TiO_2 and pH). It has been well-documented that the more O_2, OH^- adsorbed on the catalyst surface the higher the photocatalytic activity of powder samples since these species play a very important role in the photocatalytic reactions of semiconductor oxides.[21,22] Our experimental results have shown that the surface area of the samples is not the only important factor in the decomposition of RB and 2,4-DCP solutions, the difference in surface states and agglomeration states between two sets of TiO_2 samples may also be crucial factors. From the SEM images [Fig. 3(a,b)] we can see that the TiO_2 particles prepared by the photo-assisted sol-gel method exhibit very little particle agglomeration. These particles exhibit a regular polyhedral shape. The stacking is loose and there are many pores among the particles. Thus, these particles can be easily dispersed into solutions and adsorb H_2O, O_2, *etc.*, more effectively. For the P-600 sample, although its BET surface area is smaller than that of the N-500 sample the adsorption capability of the former is 2 times higher than that of the latter, which has been demonstrated by adsorption of RB and 2,4-DCP solutions in our experiments. This result most likely originates from the difference in the agglomerated states of the two sets of samples. As for the non-irradiated samples [Fig. 3(c,d)], the powders show a ceramic-like agglomeration and thus could not be well-dispersed into solutions, resulting in the lost of effective surface area. These particles are irregular and the boundaries among the particles are blurred, such that the amount of O_2, H_2O, OH^-, *etc.*, adsorbed on the surface is small, leading to a poor photocatalytic activity of the rutile particles. This experimental result further confirms that one of the fundamental reasons of the

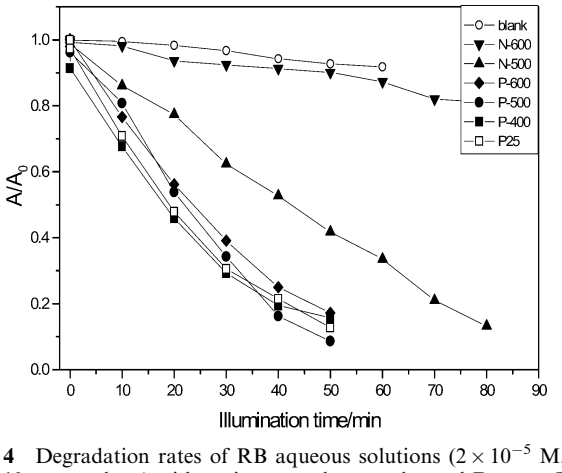

Fig. 4 Degradation rates of RB aqueous solutions (2×10^{-5} M, 50 mL, 10 mg catalyst) with various powder samples and Degussa P25: (○) blank, (▼) N-600, (▲) N-500, (◆) P-600, (●) P-500, (■) P-400, (□) P25.

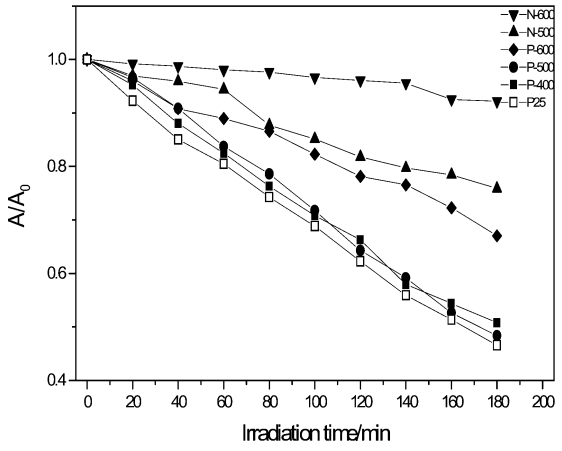

Fig. 5 The variation in absorption spectra of 2,4-DCP *versus* irradiation time during the photodegradation process with different as-prepared powder samples: (▼) N-600, (▲) N-500, (◆) P-600, (●) P-500, (■) P-400, (□) P25. The initial conditions of the reaction system: 2,4-DCP (1×10^{-4} M), 50 mL, 10 mg catalyst .

low photocatalytic activity of rutile is its poor adsorption capacity toward O_2,[23–25] OH^-[26,27] and other activated species.

Conclusions

Very different rutile particles were prepared by using a photo-assisted sol-gel method, which showed very different microstructural and photocatalytic properties from those prepared by the traditional sol-gel method. The as-prepared rutile powder samples were obtained at a relatively low calcination temperature of 600 °C and exhibited a narrow particle size distribution. Moreover, these particles had a regular polyhedral shape and hardly displayed any particle agglomeration, which results in their high adsorption capacity. The photocatalytic activity of these rutile powders was remarkable in the decomposition of rhodamine B and 2,4-dichlorophenol under ultraviolet illumination.

Acknowledgements

We gratefully acknowledge financial support from National Science Foundation of China, Chinese Academy of Sciences and National Research Fund for Fundamental Key Projects No.973 (G19990330).

References

1 I. Willner, Y. Eichem, A. J. Frank and M. A. Fox, *J. Phys. Chem.*, 1993, **97**, 7264.
2 S. Kuwabata, R. Tsuda and H. J. Yoneyama, *J. Am. Chem. Soc.*, 1994, **116**, 5437.
3 M. Matsumura, S. Furukawa, Y. Saho and H. Tsubomura, *J. Phys. Chem.*, 1985, **81**, 1327.
4 A. Fujishima, R. X. Cai, J. Otsuki, K. Hashimoto, K. Itoh, T. Yamashita and Y. Kubota, *Electrochim. Acta*, 1993, **18**, 153.
5 J. Schwitzgebel, J. G. Ekerdt, H. Gerischer and A. Heller, *J. Phys. Chem.*, 1995, **99**, 5633.
6 H. Kawaguchi, *Environ. Technol. Lett.*, 1984, **5**, 471.
7 R. W. Matthews, *J. Catal.*, 1986, **97**, 565.
8 K. Okamoto, Y. Yamamoto, H. Tanaka, M. Tanaka and A. Itaya, *Bull. Chem. Soc. Jpn.*, 1985, **58**, 2015.
9 A. Sclafani, L. Palmisano and E. Davi, *New J. Chem.*, 1990, **14**, 265.
10 K. Okamoto, Y. Yamamoto, H. Tanaka, M. Tanaka and A. Itaya, *Bull. Chem. Soc. Jpn.*, 1985, **58**, 2015.
11 A. Sclafani, L. Palmisano and M. Schiavello, *J. Phys. Chem.*, 1990, **94**, 829.
12 U. Balachandran and N. G. Eror, *J. Solid State Chem.*, 1982, **42**, 276.
13 X. Z. Ding, Z. A. Qi and Y. Z. He, *Nanostruct. Mater.*, 1994, **4**, 663.
14 D. S. Robert and A. P. Joseph, *Am. Mineral.*, 1964, **49**, 1707.
15 H. Liu, W. Yang, Y. Ma, Y. Cao and J. Yao, *New J. Chem.*, 2002, **26**, 975.
16 Z. Hengzhong and J. F. Banfield, *J. Phys. Chem. B*, 2000, **104**, 3481.
17 P. R. Hammond, *Opt. Commun.*, 1979, **29**, 331.
18 H. K. K. Pathirana and R. A. Maithreepala, *J. Photochem. Photobiol., A*, 1997, **102**, 273.
19 T. Y. Wei and C. C. Wan, *Ind. Eng. Chem. Res.*, 1991, **30**, 1293.
20 V. Augugliaro, V. Loddo, G. Marci, L. Palmisano and M. J. Lopezmunoz, *J. Catal.*, 1997, **166**, 272.
21 A. Sclafani and J. M. Herrmann, *J. Phys. Chem.*, 1996, **100**, 13 655.
22 Z. Ding, G. Q. Lu and P. F. Greenfield, *J. Phys. Chem. B*, 2000, **104**, 4815.
23 R. I. Bickley and F. S. Stone, *J. Catal.*, 1973, **31**, 389.
24 A. H. Boonstra and C. A. H. A. Nutsaers, *J. Phys. Chem.*, 1975, **79**, 1694.
25 K. Ishibashi, A. Fujishima, T. Watanabe and K. Hashimoto, *J. Phys. Chem. B*, 2000, **104**, 4934.
26 K. Kobayatawa, Y. Nakazawa, M. Ikada, Y. Sato and A. Fujishima, *Ber. Bunsen-Ges. Phys. Chem.*, 1990, **94**, 1439.
27 R. Campostrini, G. Carturan, L. Palmisano, M. Schiarello and A. Sclafani, *Mater. Chem. Phys.*, 1994, **38**, 277.